

Network Structures of Radiation-Cross-Linked Star Polymer Gels

Linda Griffith Cima* and Stephanie T. Lopina

Department of Chemical Engineering, Massachusetts Institute of Technology, Cambridge, Massachusetts 02139

Received March 21, 1995; Revised Manuscript Received July 10, 1995*

ABSTRACT: The network structure of radiation-cross-linked solutions of star molecules is analyzed theoretically and experimentally. We synthesize gels via electron beam irradiation of aqueous solutions of high-functionality ($f > 30$) star PEO in the concentration regime where the molecules exhibit extensive overlap. The expected network properties of the resulting gels are systematically varied by using PEO stars with different arm lengths and functionalities and by adjusting the irradiation dose and initial polymer concentration. The cross-link density in these gels is analyzed three ways: (1) elastic modulus, (2) swelling equilibrium, and (3) comparison to the cross-link density of linear gels prepared in a comparable fashion. In order to predict the network structure of cross-linked star molecules from swelling, Flory's equilibrium swelling theory is modified to include a bimodal distribution of cross-link functionalities. The modified equation fits the trends in swelling behavior of the series of radiation-cross-linked star PEO gels. The apparent cross-link density of radiation-cross-linked star PEO gels obtained by physical property measurement—swelling and elastic modulus—differ from the cross-link density expected based on comparison to linear gels cross-linked under identical conditions. Cross-link densities based on the elastic modulus are lower than the expected values, suggesting that a significant fraction of elastically ineffective cross-links form between star arms within the same molecule.

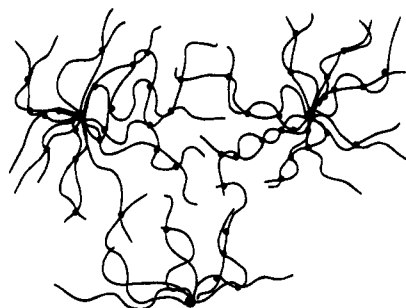
Introduction

Solvent-swollen polymer gels have been applied in a wide range of technologies including absorbents, separations media, and controlled release of pharmaceutical and agricultural agents. Applications continue to grow at a rapid pace as new methods for creating network structures are devised and relationships between structure and properties are elucidated. Synthetic star polymers offer an interesting new family of precursors for forming cross-linked gel structures, and recent advances in both synthesis and solution structure determination should enhance nascent efforts in this direction.¹

Radiation cross-linking in solution is an attractive route toward forming cross-linked networks from star polymers because it can be used to cross-link quite simple main chain chemistries such as aliphatic polyethers. These cross-linked star networks may also have a more fundamental application, though, in helping elucidate the solution properties of star polymers. Free-radical-mediated cross-linking of polymer chains in solution serves to "freeze" neighboring segments, and the resulting network structure should reflect aspects of the relative proximity of interchain and intrachain segments. In solutions of star molecules, analysis of network structures formed by radiation cross-linking may allow corroboration of light- and neutron-scattering evidence that in the semidilute regime, the arms of star polymers freely interpenetrate and behave essentially as solutions of linear molecules.^{2,3}

Many of the technologically important properties of gels, such as the permeability to solutes, elastic modulus, and the average length of dangling chain ends which can be functionalized with specialized chemical groups, are functions of the network structure. The structure of a gel network formed by radiation-induced cross-linking of star molecules will fall between two

case 1: intra-star crosslinks dominate



case 2: inter-star crosslinks dominate

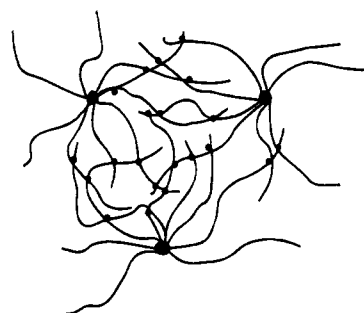


Figure 1. Two extremes of network structure expected from radiation-induced cross-linking of star polymer solutions.

extremes depicted in Figure 1. At one extreme, cross-links are formed primarily between arms of the same star molecule, with few star-star cross-links. This behavior is expected if the stars essentially repel each other in solution. At the other extreme, the dominant mode of cross-linking is star-star, resulting from free interpenetration of the arms of adjacent star molecules in solution. Assuming that chains of neighboring stars interpenetrate freely at concentrations above a critical concentration, it should be possible to obtain both extremes of network behavior by varying the weight concentration ω_p of a particular star molecule in the cross-linking solution or, alternatively, by varying the

* Author to whom correspondence should be addressed.

† Abstract published in *Advance ACS Abstracts*, August 15, 1995.

arm molecular weight, M_a , at constant star functionality, f , and ω_p . For identical cross-link concentrations, these two structures are expected to yield different properties. Dominance of star–star cross-linking should result in a higher elastic modulus and lower permeability to solutes.

We consider here in particular the case of electron-beam-induced cross-linking of poly(ethylene oxide) (PEO) stars in aqueous solution under conditions where the stars are predicted to overlap almost up to the core. The mode of cross-linking in this system is recombination of carbonyl radicals generated along the backbone to yield intersegment C–C bonds.⁴ This system is well suited to these studies because cross-linking can be carried out under conditions where chain scission and side reactions are minimal. The resulting materials have a range of potential applications, especially in the area of biomaterials. PEO exhibits an unusual degree of inertness toward the biological environment, and there is intense interest in new PEO-based materials for drug delivery, tissue engineering, and other implants.^{5–9} Cross-linked PEO star gels are particularly interesting because they offer a high concentration of terminal hydroxyl groups which can be functionalized with drugs or other moieties. They are particularly well-suited as substrates for immobilizing ligands such as proteins, peptides, and carbohydrates to engender specific interactions with cell surface receptors. Other approaches to network formation generally leave few chain ends free for ligand modification. We have used these gels and other PEO gels as substrates for immobilizing carbohydrate moieties which interact with the hepatic asialoglycoprotein receptor and found that cell response is altered by the ligand tether length.¹⁰

Our goal is to synthesize gels from solutions of star PEO which exhibit extensive overlap and thus (presumably) behave as linear molecules and compare the resulting behavior to gels made from linear PEO under similar conditions. We use measurements of equilibrium swelling and elastic modulus to assess the nature of the cross-linked structures with the aim of predicting the cross-link density and the average molecular weight between cross-links, M_c . Flory's theory of affine swelling of network structures¹¹ and its modifications^{12,13,21} provide a suitable basis for predicting these network parameters based on equilibrium swelling measurements for linear gels with homogeneous cross-link functionalities. For star polymers, we modify Flory's network swelling theory to apply to the case of cross-linked stars and predict the cross-link density based on the modified theory. We compare these results to those obtained by the elastic modulus and to what would be expected if star PEO gels formed an identical number of cross-links as linear gels cross-linked under comparable conditions.

I. Theory

The theoretical development is in two parts. First, we analyze the solution behavior of PEO stars in the semidilute regime to predict the degree of overlap of adjacent stars as a function of concentration and of the star properties f and M_a . Then, we develop a model for equilibrium swelling of radiation-cross-linked stars which relates the experimentally measured swelling ratio and star structure (as characterized by f and M_a) to the number of cross-links per star arm.

Prediction of Overlap Regimes for PEO Stars. We expect the network structure obtained by radiation cross-linking to depend on the degree of interpenetration

of adjoining stars, and thus we need a quantitative relationship between the concentration of PEO stars in aqueous solution and the expected degree of arm overlap.

In dilute solutions, the behavior of stars deviates significantly from linear molecules. The Daoud–Cotton model describes a star in terms of three regions: an extended core of meltlike segments, an intermediate region where the chains are ideal and concentrated, and an outer region where the chains are semidilute.¹⁴ The chains are considered as a string of blobs of diameter $\xi(r)$, where $\xi(r)$ increases with distance r from the center.

Experimental and theoretical results^{15–17} support a model in which the outer semidilute regime dominates, and an asymptotic scaling of the segment density ρ as a function of r for stars with $f > 30$:

$$\rho(r) \propto f^{(3\lambda-1)/2\lambda} r^{(1-3\lambda)/\lambda} \quad (1)$$

For a star of specified functionality f this scaling law can be written

$$\rho(r) = A(r/a_s)^{1/\lambda} r^{-3} \quad (2)$$

where a_s is the statistical segment size. The exponent λ has the value $3/5$ for a good solvent and thus applies for the PEO–water system. This same scaling dependence on r has been verified by self-consistent field analysis of polymer chains in a good solvent attached at high densities to spherical interfaces.¹⁸ Equating the segment density at the core–corona boundary leads to a quantitative value for the scaling prefactor: $A = 3 \times 4^{1/\lambda} f^{(3\lambda-1)/2\lambda} / 32\pi$.

Near the overlap regime, experimental evidence for star–star repulsion and liquid-like ordering has been reported.² At higher concentrations, in the semidilute range, extensive overlap between stars is predicted.^{14,19} This overlap has been demonstrated experimentally. Furthermore, light scattering and neutron scattering studies have shown that solutions of stars in the semidilute regime exhibit static and dynamic behavior similar to solutions of linear chains at the same concentration.^{2,3}

The extent to which the arms of adjacent stars interpenetrate can be estimated by equating the local segment density with the average concentration in solution¹⁴ and solving for the radius R_0 corresponding to the boundary between the more concentrated core region and the bulk. A schematic of the segment density as a function of the distance from the star core for overlapping stars is shown in Figure 2. For the case of extensive overlap, denser core regions are just small perturbations in bulk average concentration and the equality is simply

$$10^{-21} \omega_p N_a / M_m = A(R_0/a_s)^{1/\lambda} R_0^{-3} \quad (3)$$

where N_a is Avogadro's number and M_m is the molecular weight of a single monomer unit. ω_p is in g/mL, and r and a_s are in nm. For PEO, $M_m = 44$ and $a_s = 2.0$ nm.²⁰ This is the regime in which we should form cross-linked structures if the behavior can be analyzed by the modified swelling theory described below, because that theory pertains to networks with a homogeneous segment density. For a star with specified f and M_a , the appropriate ω_p to achieve essentially complete overlap of stars can be estimated by setting R_0 approximately equal to the size of the core. At lower concentrations

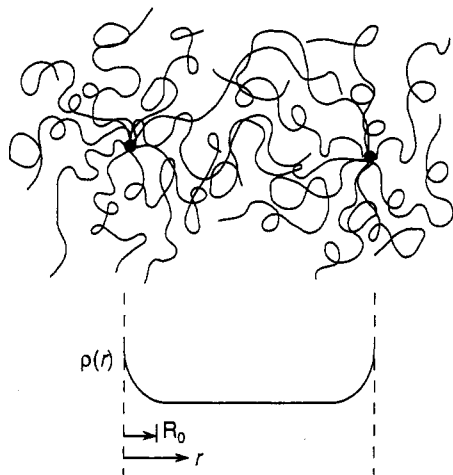


Figure 2. Local segment density as a function of distance r from the star center in semidilute solutions. At R_0 , the local segment density is equal to the average bulk concentration and the stars interpenetrate up to this distance.

(and thus less extensive overlap), contributions to the total concentration from the nonoverlapping, excluded regions and the overlapping, bulk regions contributions must be considered separately. Thus the "bulk" concentration on the left-hand side of eq 3 is corrected for the presence of denser cores and the equality becomes

$$10^{-21} \frac{\omega_p}{M_m} - \frac{\omega_p N_a}{M_{star}} \int_0^{R_0} 4\pi r^2 \rho(r) dr = \rho(R_0) \quad (4)$$

$$1 - \frac{\omega_p N_a}{M_{star}} \frac{4\pi R_0^3}{3}$$

Derivation of the Swelling Equation for Cross-Linked Star Networks. The swelling behavior of hydrogel networks has been investigated for many years. The network structure (cross-link concentration, μ , and molecular weight between cross-links, M_c) of networks which possess a low volume fraction of polymer, homogeneous F -functional junctions, and low or moderate degrees of cross-linking can be predicted using the analysis of equilibrium swelling based on Flory's development modified by Peppas, Bray, and Merrill for swelling of networks formed in the presence of a diluent^{11,12,21}

$$\frac{1}{M_c} = \frac{2}{M_n} - \frac{\frac{v_p^*}{V_1} [\ln(1 - v_{2s}) + v_{2s} + \chi_1 v_{2s}^2]}{v_{2r} \left[\left(\frac{v_{2s}}{v_{2r}} \right)^{1/3} - \frac{2}{F} \left(\frac{v_{2s}}{v_{2r}} \right) \right]} \quad (5)$$

where V_1 is the molar volume of the solvent, v_{2r} and v_{2s} are the volume fractions of polymer in the solution during irradiation and following equilibrium swelling, respectively, and v_p^* is the specific volume of the polymer. This result cannot be applied directly to radiation-cross-linked star gels because they contain a bimodal distribution of cross-link functionalities—tetrafunctional junctions induced by radiation and f -functional junctions at the star cores. Under the assumption that the arms of the star molecules behave as Gaussian chains, this result can readily be modified to account for a bimodal cross-link distribution.

To account for bimodal cross-link functionalities, we follow Flory's original development,¹¹ in which a network is formed from ν chains joined into $2\nu/F$ junctions,

where F is the junction functionality (commonly, 4). Flory gives the probability that all ν chains will be joined into $2\nu/F$ groups as

$$\Omega = \left(\frac{F\Delta\tau}{V} \right)^{2\nu(F-1)/F} \left[\left(\frac{2\nu}{F} \right)! \right]^{F-1} \quad (6)$$

where $\Delta\tau$ is the volume increment and V is the total volume of the system containing all the ν chains.

For a bimodal distribution of cross-link functionalities, we assume that the network is formed in two steps: formation of star cores followed by formation of tetrafunctional radiation-induced cross-links. The network ultimately consists of internal subchains which are joined to the network at both ends and free terminal ends. In the cross-linked star system the number of free terminal ends is assumed equal to the number of ends of star arms, ν_s , since the joining of two free arm ends by radiation is likely to be a rare event.

To describe the formation of the cross-linked star network, let ν_0 denote the total number of pairs of ends linked to junctions and $\nu_s/2$ the pairs of free chain ends. The total number of chains is thus $\nu_0 + \nu_s/2$. The first step is formation of ν_s/F_2 star cores from a subset of all available ends, $2\nu_0 + \nu_s$. The tetrafunctional links (designated by F_1 for generality) are then formed from a subset of the remaining ends. The total probability thus becomes

$$\Omega = \frac{\left[\left(\frac{2(\nu_0 + \nu_s/2)}{F_2} \right)! \right]^{F_2-1} \left[\left(\frac{2\nu_0}{F_1} \right)! \right]^{F_1-1}}{\left[\left(\frac{2\nu_0}{F_2} \right)! \right]^{F_2-1} \left[\left(\frac{\nu_s}{F_1} \right)! \right]^{F_1-1}} \left(\frac{F_2\Delta\tau}{V} \right)^{\nu_s(F_2-1)/F_2} \left(\frac{F_1\Delta\tau}{V} \right)^{2(\nu_0 - \nu_s/2)(F_1-1)/F_1} \quad (7)$$

Derivation of the entropy and enthalpy of network formation and swelling then follows directly from the development of Flory¹¹ and Peppas, Bray, and Merrill.^{12,21} The resulting expression for the change in free energy of the network ΔG with respect to change in the number of solvent molecules n_1 during swelling becomes

$$\frac{1}{kT} \frac{\partial \Delta G}{\partial n_1} = \chi_1 v_{2s}^2 + \ln(1 - v_{2s}) + v_{2s} + \left(\nu_0 - \nu_s/2 \right) \frac{V_1}{V_r} \left[\left(\frac{v_{2s}}{v_{2r}} \right)^{1/3} - \left(\frac{2}{F_1} + \frac{\nu_2}{(\nu_0 - \nu_s/2)F_2} \right) \frac{v_{2s}}{v_{2r}} \right] \quad (8)$$

where V_r is the total volume of the solution which undergoes irradiation. This reduces to Flory's equation when $F_1 = F_2$ or $\nu_s = 0$ (all chains are in F_1 -functional linkages). The effect of the bimodal cross-linking distribution is seen in the coefficient of the last term in brackets in eq 8

$$\frac{2}{F_1} + \frac{\nu_s}{(\nu_0 - \nu_s/2)F_2}$$

which represents the sum of the relative numbers of F_1 - and F_2 -type cross-links in the gel. For a gel with a single cross-link functionality F , the value of this term varies from 0.5 to zero as F increases from 4 to infinity. For gels with bimodal cross-link functionalities, the value will fall in between the two extremes. For cross-linked gels of highly functional stars ($f > 20$), the value of this coefficient will be dominated by the F_1 term if

gels are made with at least one cross-link per arm. Equation 8 can be cast in terms of the molecular weight between cross-links, M_c , by recognizing that $(\nu_0 - \nu_s/2) = (\nu_0 + \nu_s/2)(1 - M_c/M_a)$ and $\nu_0 + \nu_s/2 = V_p/(\nu_p^* M_c)$, where V_p is the total volume of polymer added to the cross-linking solution. The derivative is zero at equilibrium; thus, the final result is

$$\frac{1}{M_c} = \frac{1}{M_a} - \frac{\nu_p^*}{\nu_{2r} V_1} \frac{\chi_1 \nu_{2s}^2 + \ln(1 - \nu_{2s}) + \nu_{2s}}{\left(\frac{\nu_{2s}}{\nu_{2r}}\right)^{1/3} - \left(\frac{2}{F_1} + \frac{1}{(M_a/M_c - 1)F_2}\right) \nu_{2s}} \quad (9)$$

The result is implicit in M_c due to the effects of the bimodal cross-link distribution. With the equation in this form, it can clearly be seen that the swelling behavior is dominated by the F_1 -functional cross-links for gels comprising highly functional stars with at least one F_1 cross-link per arm. Consider a gel formed from 20-arm stars ($F_2 = 20$), cross-linked once per arm ($X_a = M_a/M_c - 1 = 1$; X_a denotes the average number of cross-links per star arm). The value of $2/F_1$ is 10 times higher for this gel than the value of the counterpart F_2 term. As the number of cross-links per arm is increased for this example, the relative number of F_2 linkages becomes even smaller and the swelling behavior appears even more like that of a gel containing only F_1 linkages.

We also derive information about the cross-linked structure of the network from the elastic modulus, which provides an independent estimate of the concentration of elastically effective chains in the network, ν_E , and the concentration of cross-links, μ_E . The elastic behavior of networks falls between two idealized limits, affine and phantom, which relate the network structure to the elastic deformation under applied stress.²²

In the affine model, network junctions (cross-links) are assumed to be affine with respect to macroscopic strain and fluctuations of the junctions are completely suppressed. This leads to an affine relationship between strain and chain end-to-end vectors,

$$E_{G,\text{affine}} = \frac{\sigma}{\lambda - \lambda^{-2}} = \nu RT \quad (10)$$

where $E_{G,\text{affine}}$ is the modulus, σ is the nominal stress, and λ is the elongation. For networks formed in the presence of solvent and then swollen further, this relationship becomes

$$E_{G,\text{affine}} = \nu_E \nu_{2r}^{-1/3} \nu_{2s}^{1/3} RT \quad (11)$$

where ν_E is the concentration of elastically effective chains in the unswollen state immediately after cross-linking.

The phantom model supposes that the chains are immaterial or "phantom" and can freely cross each other. The chains exert forces on the junctions, which are free of constraints and can thus move independently of the stress. This leads to a chain vector distribution which is a convolution of the mean chain distribution with the fluctuation distribution. The resulting theory predicts a lower elastic free energy and modulus than the affine case,

$$E_{G,\text{phantom}} = \frac{\sigma}{\lambda - \lambda^{-2}} = (\nu - \mu)RT \quad (12)$$

For networks formed in the presence of solvent this

becomes

$$E_{G,\text{phantom}} = (\nu_E - \mu_E) \nu_{2r}^{-1/3} \nu_{2s}^{1/3} RT \quad (13)$$

The behavior of real networks falls between the affine and phantom limits. For a network with only one type of cross-link, $\nu_E - \mu_E = \nu_E(1 - 2/F)$. As $F \rightarrow \infty$, the phantom model approaches the affine model. For the bimodal cross-link distributions obtained in radiation-cross-linked star gels, $\nu_E - \mu_E = \nu_E[1 - (2/F_1 + 1/(M_a/M_c - 1)F_2)]$. As with swelling behavior, we expect the elastic behavior to be dominated by the F_1 cross-links for gels formed with highly functional stars containing at least one F_1 cross-link per star arm.

The behavior of real networks can be described by including terms to reflect partial suppression of junction fluctuations and by the contribution of physical chain entanglements.²² Based on previous studies of swollen PEO networks,²³ we expect the gels we form to behave as phantom gels, with little suppression of junction fluctuations and chain entanglements. The relationship between the modulus and ν_E allows the number of cross-links and the molecular weight between cross-links to be calculated and compared to results determined by swelling.

II. Experimental Investigation of Cross-Linked PEO Star Networks

The general approach we take is to generate a series of gels in which M_a , f , and expected cross-link density are varied. We then predict the number of cross-links per arm by analyzing equilibrium swelling with eq 9. Ideally, we would verify this direct prediction by direct measurement of the number of cross-links formed during irradiation. However, the cross-links have no distinguishing chemical features which allow their direct assay in an intact gel. Degradation of the ether bonds in the gel is a potential route to direct assay of the number of cross-links formed because it theoretically leads to two- and four-carbon degradation products arising from the ethylene main-chain units and the cross-linked units, respectively. Achieving complete degradation with a product spectrum that can be analyzed by HPLC is in practice quite difficult.

We thus compare the results obtained from swelling experiments to two other predictions of cross-link density. One estimate is obtained by comparing the number of cross-links formed in the star gels to linear gels cross-linked under identical conditions (i.e., same polymer concentration and same radiation dose). In addition, we measure the elastic modulus of a subset of gels and determine bounds on the cross-link density using the affine (eq 11) and phantom (eq 13) limits. The first comparison is valid provided the solutions of star polymers behave as solutions of linear polymers at similar concentrations with respect to the cross-linking reaction. Radiation cross-linking of star PEO may be less effective than radiation cross-linking of linear PEO if the chain mobility of the stars is reduced compared to linear, thus decreasing the probability that an active main-chain radical will find another main chain. The observations that the dynamic properties of star chains are similar to those of linear chains when the concentration of stars is in the overlap regime² suggest that the cross-linking behavior of linear and star PEO will be similar in the overlap regime.

Table 1. Star Polymer Characteristics

polym desig	no. of arms	arm mol wt
3210	40	3460
3498	36	10000
3509	55	10473
BS10	186	10000

Materials and Methods

Polymers and Reagents. PEO stars produced by living anionic polymerization from divinylbenzene (DVB) cores were provided by P. Rempp.^{24,25} Linear PEO of nominal molecular weight 100K was obtained from Polysciences as a powder containing approximately 1% silica added as a flowing agent. Narrow-molecular-weight gel permeation chromatography (GPC) standards in the molecular weight range 26 000–170 000 were obtained from TSK. All other chemicals were reagent grade and used without further purification. All aqueous solutions were made with water purified with a four-cartridge Milli-Q system.

Polymer Purification and Characterization. Star PEO was obtained in the form of a powder which contained traces of the initiator, naphthalene, and other impurities. Analysis of a 5% (w/v) solution of the polymer in deuterated chloroform by proton NMR revealed, in addition to the expected peaks at $\delta = 3.7$ (ether hydrogens) and $\delta = 7.3$ (aromatic hydrogens), several broad peaks in the range $\delta = 0.9$ –2.6. Impurities were removed by adsorption on activated charcoal from a 5% (w/v) solution of the polymer in MilliQ-purified water. The charcoal was precipitated from the solution by repeated centrifugation at 1200g, and the resulting clear polymer solution was dried by rotary evaporation. NMR analysis of the purified polymer revealed only the ether hydrogens and a peak at $\delta = 7.3$ arising from the hydrogens on the DVB core of the stars. A peak due to hydrogens in the terminal hydroxyl position was not detected above the noise; this peak would be <50% of the area of the aromatic hydrogens. The unassigned peaks which had been observed prior to purification were completely removed. Linear 100K PEO was purified in a similar fashion.

The molecular weight and polydispersity of linear PEO was determined by GPC in chloroform using a three-column sequence (PL-gel guard, linear, and 1000 Å) with RI detection. Data were analyzed with Perkin-Elmer Turbochrome 3 software. Values of $M_n = 29\,750$ and $M_w/M_n = 4.3$ were obtained. Stars were analyzed by light scattering and end group titration as described elsewhere.²⁴ Characteristics of the stars are shown in Table 1.

Radiation Cross-Linking. Cross-linking of aqueous polymer solutions was achieved by electron beam irradiation using a 3 MeV Van de Graaff generator source. The generator can provide up to 10 Mrad/s uniformly to a sample up to 3 in. in width, with a penetration depth of about 1 cm in aqueous PEO solutions. Radiation was delivered at a rate of 25 000 rad/s with total dose delivered ranging from 2 to 25 Mrad. PEO solutions were irradiated in 2 g aliquots measured into 60 mm clean glass Petri dishes, keeping the depth of PEO solution exposed to the beam below 3 mm to ensure that the dose received remained uniform throughout the material. The dishes were covered with standard glass Petri dish covers and the edges were sealed with Parafilm. The high radiation dose effectively sterilizes the gels and they were handled as sterile after cross-linking. The formation of hydrogen bubbles in the gel, due to recombination of hydrogen radicals, was prevented by staging the irradiation in 2 Mrad doses separated by at least 20 h, allowing the hydrogen to diffuse out of the gel. Radiation-induced chain scission and formation of side products (carbonyls, unsaturation) was minimized by degassing the polymer solution prior to the initial irradiation to remove oxygen.

The radiation doses and concentrations of polymer in the linear cross-linking experiments were varied to cover the range of conditions used in cross-linking the star solutions. Properties of the star solutions used for cross-linking are shown in Table 2, along with the overlap radius, R_0 . The average distance d_c between the cores of neighboring stars is also shown

Table 2. Properties of Star Solutions Used for Cross-Linking

polymer	M_n	f	ω_p	d_c (nm)	R_0 , nm	
					$a_s = 2$ nm	$a_s = 1$ nm
S3509	10473	55	0.07	23	1.3	3.1
			0.04	29	2.0	4.9
S3498	10000	36	0.084	19	0.9	2.1
			0.063	21	1.1	2.6
			0.046	24	1.4	3.2
S3210	3460	40	0.08	14	1.0	2.3
			0.04	18	1.6	3.8

for comparison. The volume fraction corresponding to non-overlapping regions is <2% in all cases. Thus, from the perspective of segment density, we can treat the solutions of stars as solutions of linear molecules.

Characterization of Cross-Linked Gels. Fourier transform infrared (FTIR) spectra of starting materials and dried gels obtained at a resolution of 2.0 cm^{-1} showed no significant differences; in particular, carbonyls and unsaturation were absent in the cross-linked samples. To determine the molecular weight between cross-links and the sol fraction, gels were allowed to swell in MilliQ water for 5–15 days, exchanging the swelling media daily. A reasonable estimate of the diffusion coefficient for the sol components in the gel is $\sim 10^{-8}$ – $10^{-7}\text{ cm}^2/\text{s}$,⁴ thus the gels would be essentially free of sol fraction after the swelling period. High sol fractions (>10%) were characteristic of linear and star gels formed at low radiation doses (<6 Mrad). To obtain the dry polymer weight, swollen hydrogels (devoid of sol fraction) were dried with desiccant in a 40°C vacuum oven until a constant weight was obtained. For each set of conditions, 4–6 samples prepared in identical fashion were evaluated. Elastic moduli of fully swollen gels, in the form of 1 cm diameter disks ~ 0.12 cm thick, were determined by compression testing using an Instron mechanical testing machine equipped with a 200 g tension/compression load cell and aluminum compression platen.

Results and Discussion

Cross-Linking Behavior of Linear PEO. Cross-linking of linear PEO by irradiation in aqueous solutions has been studied extensively, and the general relationships between dose, initial polymer concentration, and resulting cross-link density have been described.²⁶ The concentration of cross-links formed generally increases with increasing radiation dose and is insensitive to the polymer concentration in the cross-linking solution under many conditions. For constant v_{2r} , M_c decreases with increasing radiation dose to a limit where chains are constrained from further cross-linking; this limit for PEO in water is $M_c \approx 1700$. For a given dose, the concentration of radiation-induced cross-links does not depend on v_{2r} , provided the sol fraction is negligible, the polymer concentration is semidilute, and M_c is above the limiting value of about 1700. Thus, for a given dose, M_c increases as v_{2r} increases because the total number of cross-links formed is constant. This insensitivity of the cross-linking process to v_{2r} over the desired range makes the behavior of cross-linked linear molecules a useful reference basis for the behavior of star molecules, given the similarities in dynamic properties of linear and star molecules in semidilute solution.

The quantity we wish to derive from the linear cross-linking experiments is the concentration of radiation-induced cross-links, μ_r , formed as a function of dose and initial polymer concentration. This quantity is

$$\mu_r = (\omega_p/2)(M_n/M_c - 1)/M_n \quad (14)$$

where ω_p is the weight concentration of polymer in the

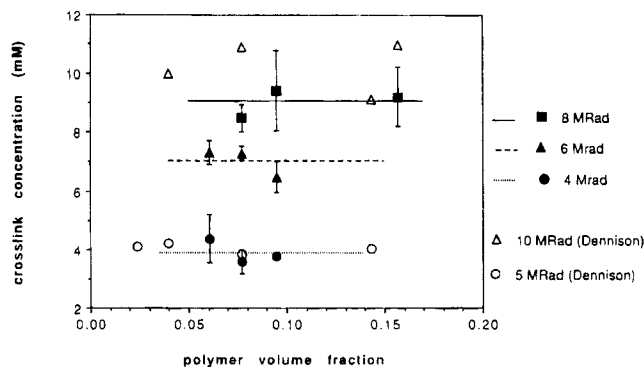


Figure 3. Concentration of cross-links formed in electron-beam-irradiated linear PEO solutions as a function of polymer volume fraction in the irradiation solution for constant doses of 4–8 Mrad.

Table 3. Elastic Moduli of Water-Swollen PEO Gels

polymer	v_{2r}	v_{2s}	dose (Mrad)	modulus (N/m ²)
linear PEO (30K)	0.143	0.030	8	7019 ± 121
BS10 (10K)	0.077	0.050	5.5	8748 ± 93
3210 (3.5K)	0.070	0.058	8	5999 ± 238

initial solution. Values of μ_r (determined from eqs 5 and 14, with values of physical constants from the literature^{4,26}) as a function of v_{2r} are shown in Figure 3 for linear gels formed at doses of 4, 6, and 8 Mrad. Some gels with $M_c < 2500$ exhibited mild (<10%) syneresis during cross-linking. These results are illustrative of the general cross-linking behavior described above. Previous data reported by Dennison²⁶ are included for comparison and are consistent with the results obtained in this study. For a given dose within the regime of interest here, μ_r is relatively insensitive to the concentration of polymer and depends on dose according to

$$\mu_r = 1.22D - 1.83 \quad (15)$$

where μ_r is in units of mM (of unswollen gel) and the radiation dose D is in Mrad.

Network Structure Derived from Elastic Properties of Linear and Star PEO Gels. The experimental results for the elastic moduli of water-swollen linear and star networks are shown in Table 3, and the values of M_c and X_a derived from the results in Table 3 are shown in Table 4. Values of M_c and X_a predicted from eq 15 for the specified dose rates are shown in Table 4 for comparison. The M_c of linear PEO gels determined by equilibrium swelling matches the M_c determined from $E_{G,phantom}$. This result is consistent with previous results reported for PEO gels.²³ A comprehensive study of model PEO networks synthesized by end-linking linear PEO chains with plurifunctional cross-linking reagents ($f = 2$ –9) demonstrated that the elastic behavior of such networks very closely approached the phantom limit for networks with a high solvent content ($v_{2r} < 0.2$) or short chains ($M_c < 4000$).²³ Behavior close to the affine limit was exhibited by networks with long chains or high volume fractions of polymer. Ferry²⁷ estimated the average M_{en} between

physical entanglements in bulk linear PEO as 2200. One would expect on average 2.9 entanglements between each cross-linked chain in the linear gels described in Table 4 ($M_c = 8500$) if they behave like bulk linear PEO. However, fewer entanglements are expected at low polymer volume fractions. Indeed, the concentration of entanglements was reported as zero²³ for PEO gels with $M_c = 5600$ and a polymer volume fraction of 0.043, a volume fraction comparable to that of the linear gels described in Tables 3 and 4.

Star gels behave differently than linear gels—the behavior falls outside the range of both the affine and phantom models. The values of μ_E derived from the elastic modulus are lower than those expected from comparison with linear gels (eq 15). The values of M_c determined from the elastic modulus are thus greater, and values of X_a lower, as shown in Table 4. Results are shown for two representative gels, one with $M_a = 10\,000$ and one with $M_a = 3460$. The values of M_c for these gels are well above the plateau regime where chains are constrained from cross-linking.

In the semidilute regime, the dynamic properties (mutual diffusion coefficients) of linear and star molecules in a good solvent are independent of chain architecture and depend only on concentration.² The probability that two main-chain radicals will encounter each other should thus be the same for solutions of linear and star molecules. Thus, there is no compelling reason that fewer cross-links would form in star gels in comparison to linear gels formed under the same conditions. The results thus suggest that a significant fraction of cross-links (about 25%) occur between two adjacent star arms, leading to unproductive “loops” in the network and to an apparent lower value of μ_E .

Swelling Behavior of Star PEO Gels. A series of gels were synthesized from PEO stars in which f was varied at constant M_a ($M_a = 10\,000$, $f = 36, 55$, and 186) and in which M_a was varied with an approximately constant value of f ($M_a = 3460$ and $10\,000$ for $f = 40$ and 36). The results of equilibrium swelling were analyzed with eq 9 using a value of χ_1 identical to that for linear PEO. Table 5 and Figure 4 summarize the results of these swelling experiments for star gels.

The values of M_c (and X_a) obtained by swelling experiments are sensitive to the value of the Flory–Huggins χ_1 interaction parameter. The χ_1 parameter in theory arises from the enthalpy of mixing of polymer segments and solvent molecules.²⁸ χ_1 appears as the only arbitrary parameter in the theoretical description of the free energy of mixing of a binary solution of polymer and solvent. Thus, when fitting experimental data to the theory, χ_1 also compensates for deficiencies in the theoretical description of the entropy of mixing.²⁸ Values of χ_1 for linear and star PEO are therefore expected to differ due to differences in both configuration and composition (stars have a hydrophobic DVB core) of the linear and star PEO molecules. The results presented in Table 5 and Figure 4 illustrate the degree of this sensitivity by comparing network parameters obtained using three different values of χ_1 —the value corresponding to linear PEO, the value which allows μ_r

Table 4. Network Structures Derived from Elastic Moduli of Water-Swollen PEO Gels

polymer	v_{2r}	$M_{c,affine}$	$M_{c,phantom}$	$M_{c,dose}^a$	$X_{a,affine}$	$X_{a,phantom}$	$X_{a,dose}$
linear PEO (30K)	0.143	10526	7468	(8517)			
BS10 (10K)	0.077	6941	4885	4737	0.44	1.05	1.16
3210 (3.5K)	0.070	3141	2876	2200	0.10	0.20	0.70

^a Obtained by using eq 15; doses are given in Table 3.

Table 5. Cross-Link Densities for Star Gels

polymer	ν_{2r}	ν_{2s}	dose (Mrad)	$X_{a,dose}^a$	X_a , from swelling ^b		M_c , from swelling ^b	
					$\chi_1 = 0.426$	$\chi_1 = 0.48$	$\chi_1 = 0.426$	$\chi_1 = 0.48$
Gels with No Syneresis								
3498 (10K)	0.085	0.063	8	1.89 ± 0.11	4.43 ± 0.39	1.94 ± 0.22	1857 ± 167	3429 ± 250
3498	0.063	0.053	8	2.55 ± 0.17	4.03 ± 0.49	1.67 ± 0.26	2006 ± 221	3778 ± 334
3509 (10K)	0.069	0.067	10	3.01 ± 0.20	6.56 ± 0.94	3.22 ± 0.58	1323 ± 185	2545 ± 287
BS10 (10K)	0.077	0.050	5.5	1.27 ± 0.12	3.30 ± 0.50	1.16 ± 0.25	2328 ± 349	4637 ± 514
3210 (3.5K)	0.081	0.063	8	0.72 ± 0.05	1.68 ± 0.19	0.73 ± 0.11	1364 ± 150	2105 ± 201
3210	0.077	0.064	8	0.75 ± 0.08	1.86 ± 0.23	0.82 ± 0.14	1277 ± 166	2007 ± 225
Gels with Syneresis								
3498	0.036	0.041	4	1.71 ± 0.09	4.59 ± 0.84	1.78 ± 0.41	1805 ± 326	3630 ± 510
3498	0.047	0.061	8	3.43 ± 0.23	8.94 ± 1.8	3.87 ± 1.22	1015 ± 254	2090 ± 402
3210	0.041	0.057	4	0.97 ± 0.06	3.21 ± 0.55	1.36 ± 0.30	867 ± 147	1546 ± 216

^a Number of cross-links based on results from linear PEO described in eq 15. ^b From eq 9.

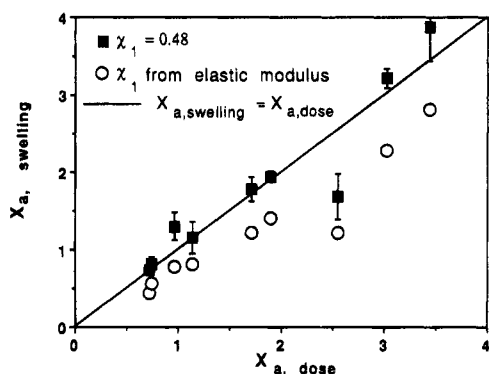


Figure 4. Relationship between predicted and measured values of the cross-link density, expressed as X_a cross-links/star arm, for PEO gels. Error bars represent standard deviations of 4–6 samples and are shown for one set of data, but are comparable for all. Results are shown for $\chi_1 = 0.48$, which gives the best fit to $X_{a,swelling} = X_{a,dose}$, and for χ_1 determined from the elastic modulus (0.49 for $M_a = 10\,000$ and 0.50 for $M_a = 3460$).

for the stars to most closely match μ_r expected from eq 15, and the value determined from the elastic modulus measurements as described above.

For linear, un-cross-linked PEO ($M_n = 35\,000$) in the volume fraction range 0.04–0.13, χ_1 has a constant value of 0.43 ± 0.01 and increases at higher concentrations.²⁶ The volume fractions of PEO in the linear gels described above are all within the range where χ_1 is constant. The value of χ_1 for the PEO star polymers used in these experiments is expected to be greater than that for linear PEO, based on previous studies by Gnanou and co-workers,²³ who formed water-swollen PEO gels formed by end-linking PEO chains ($M_w = 1000$ – $10\,000$) with pluriisocyanates. They reported χ_1 values in the range 0.45–0.58 for PEO; χ_1 values were calculated by equating the values of $\nu_E - \mu_E$ derived from equilibrium swelling to those derived from the elastic modulus. The lower bound of 0.45, which is close to the reported literature value for pure PEO in water, was obtained for gels with long chains and low polymer volume fractions. The authors reasoned that the hydrophobic urethane linkages served to increase the value of χ_1 for gels with short chains. The hydrophobic DVB cores of the stars may be acting in a similar fashion here, slightly elevating the value of χ_1 for stars relative to that for linear PEO.

χ_1 values for star PEO calculated using the M_c determined from the elastic modulus are 0.49 and 0.5 for the $M_a = 10\,000$ and $M_a = 3460$ gels, respectively. These results are well within the values reported by Gnanou *et al.* for their urethane-linked PEO gels.²³ A

higher value of would be expected for the gel with the shorter arms, as observed.

When the value of 0.43 is used for χ_1 in the calculation of M_c for the star gels from eq 9, the values are underpredicted (or, alternatively, values of X_a are overpredicted) in comparison to the values obtained by assuming the irradiated star solutions form the same number of cross-links as irradiated linear solutions for a given dose (Table 5). Results obtained with star gels for $\chi_1 = 0.43$ predict M_c values in the range of 1000 and are clearly inconsistent with the minimum M_c of about 1700 observed for linear PEO. For linear PEO, Dennison²⁶ described a plateau value of M_c with increasing dose at a constant ν_{2r} . This plateau results when the rate of chain scission is balanced by the rate of cross-linking, which decreases as the chains become more tightly cross-linked and their movement is constrained. The plateau value of M_c depends slightly on ν_{2r} and is ~ 1700 for values of ν_{2r} comparable to those in this study.

It thus seems unlikely that the results obtained for $\chi_1 = 0.43$ accurately represent the network structure of star gels. If χ_1 is viewed as an adjustable parameter used to force the values of M_c (and X_a) as determined by swelling as close to those which would be expected from eq 15 as possible, a value of 0.48 is obtained. The resulting network parameters are shown in Table 4. The results for X_a are also depicted graphically in Figure 4, as a plot of $X_{a,swelling}$ vs $X_{a,dose}$, to illustrate the agreement over the full range of X_a values. The solid line in Figure 4 indicates $X_{a,swelling} = X_{a,dose}$, and the data fit this line with a correlation coefficient of 0.877. No significant differences between gels which exhibited syneresis during cross-linking and those which did not are observed.

The most realistic values of χ_1 are those determined from the elastic modulus, which are slightly greater than 0.48 and different for stars with different arm lengths. When these values (0.49 for $M_a = 10\,000$ and 0.5 for $M_a = 3460$) are used for χ_1 in the swelling equation, values of $X_{a,swelling}$ are 25% less than values of $X_{a,dose}$. The results are plotted in Figure 4 along with the results for $\chi_1 = 0.48$. Linear regression of the resulting data gives a slightly better fit to a straight line (correlation coefficient of 0.899) than results for $\chi_1 = 0.48$.

An important observation from Figure 4 is that the correlation between $X_{a,dose}$ and $X_{a,swelling}$ is independent of X_a . Over the range of X_a corresponding to $\chi_1 = 0.48$ in Figure 4, the proportion of elastically effective chains to total chain varies from 0.4 to 0.8. Furthermore, the results for stars of different functionalities and arm

lengths also fall on the same line. The swelling model thus appears to define the concentration of elastically effective chains appropriately.

Conclusions

The network structure of radiation-cross-linked star PEO hydrogels was investigated theoretically and experimentally. The results were well described by a version of Flory's network swelling equation modified to incorporate the effects of a bimodal cross-link distribution. For hydrogels formed in the regime where extensive interpenetration of adjacent stars is expected, the results predict a lower cross-link density than expected based on results from linear gels. Based on the similar dynamic properties of linear and star molecules in the concentration range used for cross-linking and the insensitivity of the cross-linking process to polymer concentration, we conclude that apparent lower cross-link density observed for star gels results from formation of ineffective intrastar cross-links.

Formation of a significant fraction of intrastar cross-links implies that chain segments of a particular star are not distributed uniformly in the region outside R_0 shown in Figure 2. Even though the arms of adjacent stars are predicted to interpenetrate up close to the core and the solution behaves in many ways as a solution of linear molecules, the region around a particular star molecule outside R_0 in Figure 2 is perhaps enriched in segments belonging to it relative to segments belonging to adjacent stars. The technique of radiation cross-linking thus gives additional insights into the semidilute solution behavior of star molecules.

Acknowledgment. We thank Dr. Kenneth Wright of the MIT High Voltage Research Laboratory for assistance with electron beam radiation and are indebted to Prof. Paul Rempp and Pierre Lutz for a gift of characterized PEO star polymers. We thank David Weisberg for performing the mechanical testing of PEO gels. We are also grateful to Prof. Edward Merrill for his advice, interest, and many enlightening discussions about the work described here. This research was supported by NIH 1R29GM50047-01A1, NSF BCS 9157321, and the Procter and Gamble Co. S.T.L. was partially supported by an NIH predoctoral training grant.

References and Notes

- (1) Merrill, E. W.; Rempp, P.; Lutz, P.; Sagar, A.; Connolly, R.; Callow, A. D.; Gould, K.; Ramberg, K. In *Transactions of the American Society for Biomaterials*; Charleston, 1990.
- (2) Adams, M.; Fetters, L. J.; Graessley, W. W.; Witten, T. A. *Macromolecules* **1991**, *24*, 2434–2440.
- (3) Willner, L.; Jucknischke, O.; Richter, D.; Roovers, J.; Zhou, L.-L.; Toporowski, P. M.; Fetters, L. J.; Huang, J. S.; Lin, M. Y.; Hadjichristidis, N. *Macromolecules* **1994**, *27*, 3821–3829.
- (4) Merrill, E. W.; Dennison, K. A.; Sung, C. *Biomaterials* **1993**, *14*, 1117–1126.
- (5) Takahara, A.; Coury, A. J.; Hergenrother, R. W.; Cooper, S. L. *J. Biomed. Mater. Res.* **1991**, *25*, 341–346.
- (6) Hill-West, J. L.; Chowdhury, S. M.; Slepian, M. J.; Hubbell, J. A. *Proc. Natl. Acad. Sci. U.S.A.* **1994**, *91*, 5967–5971.
- (7) Yu, H.; Grainger, D. W. *Macromolecules* **1994**, *27*, 4554–4560.
- (8) Bergström, K.; Holmberg, K.; Safran, A.; Hoffman, A. S.; Edgell, M. J.; Kozlowski, A.; Hovanes, B. A.; Harris, J. M. *J. Biomed. Mater. Res.* **1992**, *26*, 779–790.
- (9) Peppas, N. A.; Langer, R. *Science* **1994**, *263*, 1715–1720.
- (10) Lopina, S. T.; Wu, G.; Merrill, E. W.; Cima, L. G. *Biomaterials* **1995**, in press.
- (11) Flory, P. J. *J. Chem. Phys.* **1950**, *18*, 108–111.
- (12) Bray, J. C.; Merrill, E. W. *J. Appl. Polym. Sci.* **1973**, *17*, 3779–3794.
- (13) Peppas, N. A.; Barr-Howell, B. D. In *Hydrogels in Medicine and Pharmacy I*; Peppas, N. A., Ed.; CRC Press: Boca Raton, 1986; Vol. 1, pp 27–56.
- (14) Daoud, M.; Cotton, J. P. *J. Phys.* **1982**, *43*, 531–538.
- (15) Vagberg, L. J. M.; Cogan, K. A.; Gast, A. P. *Macromolecules* **1991**, *24*, 1670–1677.
- (16) Grest, G. S.; Kremer, K.; Witten, T. A. *Macromolecules* **1987**, *20*, 1376–1383.
- (17) Roovers, J.; Zhou, L.-L.; Toporowski, P. M.; van der Zwan, M.; Iatrou, H.; Hadjichristidis, N. *Macromolecules* **1993**, *26*, 4324–4331.
- (18) Dan, N.; Tirrell, M. *Macromolecules* **1992**, *25*, 2890–2895.
- (19) Witten, T. A.; Pincus, P. A.; Cates, M. E. *Europhys. Lett.* **1986**, *2*, 137–140.
- (20) Lee, E. M.; Simister, E. A.; Thomas, R. K. *Mol. Cryst. Liq. Cryst.* **1990**, *179*, 151–161.
- (21) Peppas, N. A.; Merrill, E. W. *J. Polym. Sci., Polym. Chem. Ed.* **1976**, *14*, 441.
- (22) Queslel, J. P.; Mark, J. E. *Adv. Polym. Sci.* **1984**, *65*, 135–176.
- (23) Gnanou, Y.; Hild, G.; Rempp, P. *Macromolecules* **1987**, *20*, 1662–1671.
- (24) Gnanou, Y.; Lutz, P.; Rempp, P. *Makromol. Chem.* **1988**, *189*, 2885–2892.
- (25) Rempp, P.; Lutz, P.; Merrill, E. W. *Polym. Prepr. (Am. Chem. Soc., Div. Polym. Chem.)* **1990**, *31*, 215.
- (26) Dennison, K. A. Ph.D. Thesis, Massachusetts Institute of Technology, 1986.
- (27) Ferry, J. D. *Viscoelastic Properties of Polymers*, 3rd ed.; John Wiley & Sons: New York, 1980.
- (28) Flory, P. J. *Principles of Polymer Chemistry*; Cornell University Press: Ithaca, NY, 1953.

MA950391F